

1 **Effects of Urbanization on the water cycle in the Shiyang River**
2 **Basin: Based on stable isotope method**

3 Rui Li^{a,b}, Guofeng Zhu^{a,b,*}, Siyu Lu^{a,b}, Liyuan Sang^{a,b}, Gaojia Meng^{a,b}, Longhu Chen^{a,b},
4 Yinying Jiao^{a,b}, Qinqin Wang^{a,b}

5 **Affiliations:**

6 ^a *College of Geography and Environmental Science, Northwest Normal University, Lanzhou*
7 *730070, Gansu, China*

8 ^b *Shiyang River Ecological Environment Observation Station, Northwest Normal University,*
9 *Lanzhou 730070, Gansu, China*

10 **Corresponding author. Email: zhugf@nwnu.edu.cn.*

11 **Abstract:** In water-scarce arid areas, the water cycle is affected by urban
12 development and natural surface changes, and urbanization has a profound impact on
13 the hydrological system of the basin. Through an ecohydrological observation system
14 established in the Shiyang River basin in the inland arid zone, we studied the impact
15 of urbanization on the water cycle of the basin using isotope methods. The results
16 showed that urbanization significantly changed the water cycle process in the basin,
17 and accelerated the rainfall-runoff process due to the increase of urban land area, and
18 the mean residence time (MRT) of river water showed a fluctuating downward trend
19 from upstream to downstream, and was shortest in the urban area in the middle
20 reaches, and the MRT was mainly controlled by the landscape characteristics of the
21 basin. In addition, our study showed that river water and groundwater isotope data
22 were progressively enriched from upstream to downstream due to the construction of
23 metropolitan landscape dams, which exacerbated evaporative losses of river water,

24 and also strengthened the hydraulic connection between groundwater and river water
25 around the city. Our findings have important implications for local water resource
26 management and urban planning and provide important insights into the hydrologic
27 dynamics of urban areas.

28 **Keywords:** Urbanization; Water cycle; Stable isotopes; River Connectivity

29 **1 Introduction**

30 According to the "2020 Global Cities Report," urban areas are currently home to
31 more than half of the worldwide people, which amounts to 56.2%. This pattern is
32 expected to continue over the course of the next decade, culminating in an
33 urbanization rate of 60.4% by the year 2030. In addition, the study forecasts that by
34 the year 2050, approximately seventy percent of the world's population would reside
35 in urban areas (Chen et al., 2020; UN, 2019; UN-Habitat, 2020). Unlike other regions,
36 urban regions have a substantial influence on the hydrological system, resulting in
37 significant consequences on water balance and the water cycle (Gillefalk et al., 2021).
38 To meet the diverse household and industrial requirements in metropolitan areas,
39 where the population is concentrated and water demands are high, a complex
40 interplay between natural and manmade components of the water cycle is required.
41 These components include both natural features such as streams and groundwater, as
42 well as human-made systems like drinking water and drainage networks (Gessner et
43 al., 2014). Urbanization exacerbates water depletion and has far-reaching impacts on
44 groundwater (Flörke et al., 2018; McDonough et al., 2020), affecting the environment
45 and water availability (Bhaskar and Welty, 2015). Rapid urbanization will seriously

46 pressure the structure, function and water quality degradation of basin ecosystems
47 (Grimm et al., 2008; Sun and Lockaby, 2012; Sun et al., 2015).

48 Urbanization's effects on basin hydrology and the related processes have
49 complex and varying consequences (Caldwell et al., 2012; Martin et al., 2017). In the
50 past few decades, with the continuous acceleration of urbanization, human activities
51 in urban areas have become more frequent, and the hydrological effects of
52 urbanization have become more intense, attracting widespread attention worldwide
53 (Salvadore et al., 2015). The rise of impervious surfaces in urbanized regions
54 increases the rate of urban water runoff, which raises the danger of urban floods
55 (Wing et al., 2018). In addition, high-intensity human activities have led to increased
56 discharge of domestic sewage and industrial wastewater, deteriorating water quality
57 and ecological environment (Pickett et al., 2011). Meanwhile, basin water cycle
58 processes are influenced by a combination of meteorological and subsurface factors. It
59 has been found that urbanization has led to significant increases in runoff and peak
60 flows in rivers (Liu et al., 2018; Han et al., 2022) and has resulted in shorter runoff
61 response times (Anderson et al., 2022), which also exacerbates the intensity and
62 frequency of flooding in basins (De Niel and Willems, 2019; Blum et al., 2020). On
63 the other hand, the urbanization process leads to an increase in the amount of rainfall
64 in the basin as well as an increase in the frequency of extreme rainfall events (Shastri
65 et al., 2015; Fu et al., 2019; Yang et al., 2021), whereas in dryland inland river basins
66 in arid zones that are dependent on water resources for development, the impacts of
67 urbanization on the water cycle processes of the basins are still not clear, and they

68 need to be explored in depth the effects of urbanization on basin water cycle processes.

69 Hence, study into how human activities alter the features of river runoff and the water
70 cycle within a basin is essential for the prudent use and sustainable development of
71 water resources.

72 Isotopes that are stable of hydrogen and oxygen are very useful tools for
73 investigating hydrological issues that are connected to surface water and groundwater
74 sources (Fekete et al., 2006; Förstel and Hützen, 1983; Vystavna et al., 2021).

75 Researchers have been conducting studies using stable isotopes as tracers over the
76 course of the past few years in order to explore the impact that urbanization has had
77 on the water cycle. Urbanization has the potential to trigger and intensify convective
78 activity and warm-season rainfall in both urban areas and their surrounding regions
79 (Burian and Shepherd, 2005). Researchers generally agree that urbanization reduces
80 depressions on the underlying surface, weakens water permeability and increases
81 runoff. At the same time, the lower roughness of the underlying surface shortens the
82 confluence time (Guan et al., 2015; Oudin et al., 2018). Moreover, against the
83 backdrop of swift urbanization, the swift proliferation of urban regions has resulted in
84 a sharp surge in impermeable areas, alterations to regional microclimates, and the
85 erection of a vast number of infrastructures (including overpasses, subways, and so
86 on), all of which have significantly impacted the water cycle process in urban areas
87 (Jacobson, 2011; Westra et al., 2014). The complex connection between the permeable
88 and impermeable zones influences the surface confluence processes (Brouwier et al.,
89 2020). The construction of urban water conservation projects, such as rubber dams

90 and pumping stations, also affects the confluence process of urban areas to a certain
91 extent (Zhu et al., 2021). Limited long-term and continuous monitoring has hampered
92 accurate depiction of urbanization's spatiotemporal effects on basin hydrology.
93 Furthermore, the scientific research till lacks sufficient research on arid regions that
94 heavily depend on mountain river runoff for sustenance and development.

95 **Against the background of increasing urbanization, it is particularly important to**
96 **study the hydrological impacts of urbanization on basins and their corresponding**
97 **countermeasures, especially in arid inland river basins, where the impacts of human**
98 **activities in urban areas on rivers may be more prominent. Therefore, the Shiyang**
99 **River Basin (SYR), located in the inland arid zone of Northwest China, was used as**
100 **an example to study the impact of urbanization on the hydrology of the basin using**
101 **the stable isotope method.** The following problems are proposed to be solved: (1) An
102 examination of the mechanisms underlying evaporation and infiltration of surface
103 water within urban aquatic ecosystems; (2) Assessing the effects of urbanization on
104 water body connectivity through a comprehensive analysis; (3) The influence of
105 urbanization on the precipitation-runoff process is analyzed. This provides us with
106 essential information on how to maintain and manage the water resources found in
107 inland river basins, which is especially useful in light of the fact that the rate of
108 urbanization is growing.

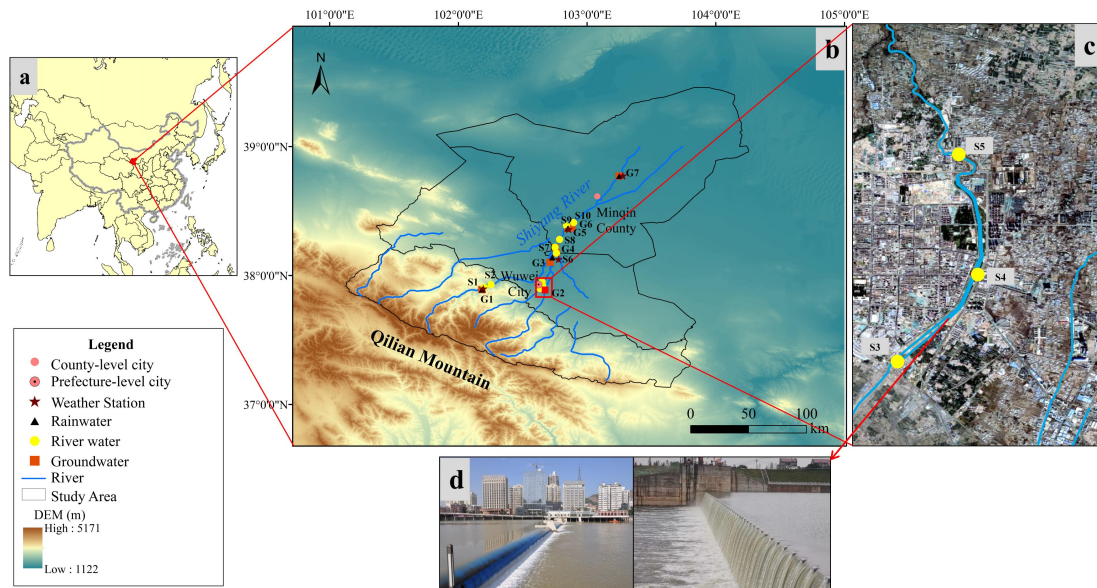
109 **2 Systems, Data, and Methods of Observation**

110 The SYR Basin is located in Gansu Province, China, to the east of the He-xi
111 Corridor. Its coordinates are 101°22' ~ 104°16' E and 36°29' ~ 39°27' N. The SYR

112 Basin is bounded to the west by the Wushaoling Mountain and to the north by the
113 foothills of the Qilian Mountain (Zhu et al., 2019). The basin in question is situated
114 within the continental temperate belt, characterized by a parched climate and diverse
115 topography. Annual precipitation hovers within the range of 100 to 600 mm, while
116 pan evaporation levels exhibit greater variability, ranging from 700 to 2600 mm
117 annually. The majesty of the Qilian Mountains is where the SYR begins its journey,
118 and the Qilian Mountains are the source of its eight main tributaries. The SYR is
119 principally supported by the convergence of precipitation, snowmelt, and glacier
120 runoff (Wei et al., 2013).

121 The Wuwei City is crossed by four important rivers, namely the Xiying, Zamu,
122 Huangyang and Jinta, which cover a catchment area of 3986 km². As the principal
123 water source for the entire region, the SYR Basin is one of the most highly utilized
124 inland river basins in terms of water resource development and consumption
125 worldwide. The dams in the SYR basin are predominantly situated in close proximity
126 to the urbanized regions of Liangzhou District, located within Wuwei City. Liangzhou
127 District, situated in the middle of the basin, boasts of a relatively high population
128 density and a notable commercial concentration. At the turn of the millennium,
129 Wuwei City only boasted a paltry five landscape dams positioned on its rivers. As of
130 2019, this figure has surged dramatically, with a staggering total of 51 urban
131 landscape dams now gracing both urban and peri-urban areas of the city. These dams
132 are primarily composed of man-made landscape waterfalls and rubber dams, fulfilling
133 their core function of creating public landscape water bodies within the urban expanse.

134 (Zhu et al ., 2021).



135

136 Figure 1 (a) The location of the study area, (b) Comprehensive observation system for the study
137 area, (c) Urban surface water sampling points (from Google Maps), (d) Common urban landscape
138 dams in SYR Basin.

139 3 Sampling and data analysis

140 Since 2017, a comprehensive observation system has been established in the
141 SYR Basin, and stable isotope observations and hydrometeorological observations
142 have been carried out on surface water, shallow groundwater and rainfall. Continuous
143 sampling in the SYR Basin was carried out from April 2017 to March 2021, different
144 water bodies were sampled, and we collected a total of 943 samples from 24 sampling
145 points (Table 1). The river sampling location ought to be selected such that it is
146 physically possible to go as close to the middle of the river as possible, with the goal
147 of minimizing the impact of areas with standing water and sewage. Artesian well
148 water was collected as groundwater samples at 7 sampling locations around the basin.
149 The automated weather station was used to measure meteorological factors such as

150 temperature and relative humidity while collecting precipitation samples. Water
 151 samples were sealed in high-density polyethylene bottles to avoid evaporation and
 152 leakage during transit and storage, precipitation samples were collected using weather
 153 station standard rain gauges. These samples were then frozen and wrapped with
 154 plastic tape.

155 Table 1 Basic information on precipitation, surface water and groundwater sampling sites

Parameter	Sampling Point	Number	Sampling period	Collection Channels
Precipitation	P1, P2, P3, P4, P5,P6, P7,	387	Precipitation events	Rain tube collection
Surface Water	S1,S2,S3,S4,S5,S6, S7, S8, S9, S10	270	Monthly	Sampling in river water
Groundwater	G1, G2, G3, G4, G5, G6, G7	189	Monthly	Sampling from wells

156 Analysis of the water samples is conducted through liquid water isotope
 157 analysis utilizing the DLT-100 (Los Gatos Research) in the Stable Isotope Laboratory
 158 at Northwest Normal University. Each water sample and isotope standard are injected
 159 six times in succession to assure reliable findings, with the first two injection values
 160 eliminated and the average of the last four injections used for final analysis, thereby
 161 avoiding any potential isotope analysis memory effect. The isotope measurements
 162 were denoted by the symbol " δ ," which indicates the deviation in thousandths from
 163 the Vienna Standard Mean Ocean Water:

$$164 \quad \delta_{\text{sample}}(\text{‰}) = \left[\left(\frac{R_s}{R_{v-smow}} \right) - 1 \right] \times 1000 \quad (1)$$

165 where R_s is the ratio of $^{18}\text{O}/^{16}\text{O}$ or $^2\text{H}/^1\text{H}$ in the collected sample, R_{v-smow} is the

166 ratio of $^{18}\text{O}/^{16}\text{O}$ or $^2\text{H}/^1\text{H}$ of the Vienna standard sample, and the analytical accuracy
167 of δD and $\delta^{18}\text{O}$ is $\pm 0.6\text{‰}$ and $\pm 0.2\text{‰}$, respectively.

168 **3 Analysis methods**

169 **3.1 Calculation and indication of *d-excess***

170 Dansgaard (1964) introduced the concept of deuterium excess (*d-excess*) as the
171 difference in isotopic composition between global precipitation and the Vienna
172 Standard Mean Ocean Water (V_{SMOW}) reference water, which corresponds to a value of
173 10‰. This parameter reflects the average isotopic composition of air masses
174 associated with precipitation and is widely used to identify atmospheric source
175 regions (Deng et al., 2016). *d-excess* was proposed by Dansgaard (Dansgaard, 1964)
176 and is defined as:

$$177 \quad d\text{-excess} = \delta\text{D} - 8\delta^{18}\text{O} \quad (2)$$

178 **3.2 Calculation of evaporation losses of surface water**

179 The losses of surface water through evaporation and the resulting fluctuations in
180 water levels of rivers, lakes, and wetlands are key aspects of the terrestrial water cycle
181 that merit significant attention (Gammons et al., 2006; Hamilton et al., 2005).
182 Evaporation is the primary mechanism of water losses in the water cycle. For river
183 water in dry regions and urban river water that flows slowly due to manmade
184 constraints, evaporation cannot be ignored. Thus, it is vital to address the alteration of
185 urban landscape dam water caused by non-equilibrium isotope fractionation during
186 evaporation. The provided formula (3) can be used to estimate the rate of evaporative
187 water losses from the body of water in question (Skrzypek et al., 2015):

$$f = 1 - \left[\frac{(\delta - \delta^*)}{(\delta_0 - \delta^*)} \right]^{\frac{1}{m}} \quad (3)$$

188

189 The variables in the equation are as follows: f represents the ratio of water lost to
 190 evaporation, δ denotes the measured values of the water body located in the urban
 191 dam area of Wuwei City, situated in the middle reaches of the SYR and δ_0 represents
 192 the initial value of the hydrogen and oxygen stable isotope of the water body. It is
 193 widely assumed that the point of intersection between the local meteoric water line
 194 (LMWL) and the local evaporation line (LEL) represents the average isotopic
 195 composition of the input water body within the basin (Gibson et al., 2005). In the
 196 current investigation, the intersection point marked by $\delta^{18}\text{O} = -7.24\text{‰}$ and $\delta\text{D} =$
 197 -46.9‰ has been designated as the δ_0 value, while δ^* denotes the maximum isotope
 198 enrichment factor and m corresponds to the enrichment slope. The calculation of the
 199 above parameters in this paper is realized in Hydrocalculator software (Skrzypek et al.,
 200 2015) (<http://hydrocalculator.gskrzypek.com>). According to studies (Qian et al., 2007),
 201 it is more accurate to use $\delta^{18}\text{O}$ when calculating the evaporation losses ratio, so this
 202 study calculates the f value of SYR water using $\delta^{18}\text{O}$ value.

203 3.3 Periodic regression analysis and the mean residence time (MRT)

204 Seasonal fluctuations in $\delta^{18}\text{O}$ values were analyzed using periodic regression
 205 analysis to determine how these values changed over time. This method entailed
 206 fitting seasonal sine wave curves to annual $\delta^{18}\text{O}$ variations using least squares
 207 optimization (Rodgers et al., 2005):

208

$$\delta^{18}\text{O} = \delta^{18}\text{O}_{ave} + A \cdot [\cos(c \cdot t - \theta)] \quad (4)$$

209 The modelled $\delta^{18}O$ values and the mean weighted annual measured $\delta^{18}O_{ave}$
210 values were both utilized in the analysis of seasonal fluctuations in $\delta^{18}O$ levels.
211 Additionally, the measured $\delta^{18}O$ annual amplitude (A), the radial frequency of annual
212 fluctuations (c), and the time in days after the start of the sampling period (t) were
213 also considered in this analysis. Furthermore, the phase lag or time of the annual peak
214 $\delta^{18}O$ in radians (θ) was determined through this approach.

215 An exponential model was used for the purpose of estimating the mean residence
216 time (MRT). This model operates on the presumption that precipitation inputs quickly
217 mix with resident water. In order to do this, the following equation was used
218 (Maloszewski et al., 1983; Rodgers et al., 2005):

$$219 \quad MRT = c^{-1} \cdot \left[(A_{Z2} / A_{Z1})^{-2} - 1 \right]^{0.5} \quad (5)$$

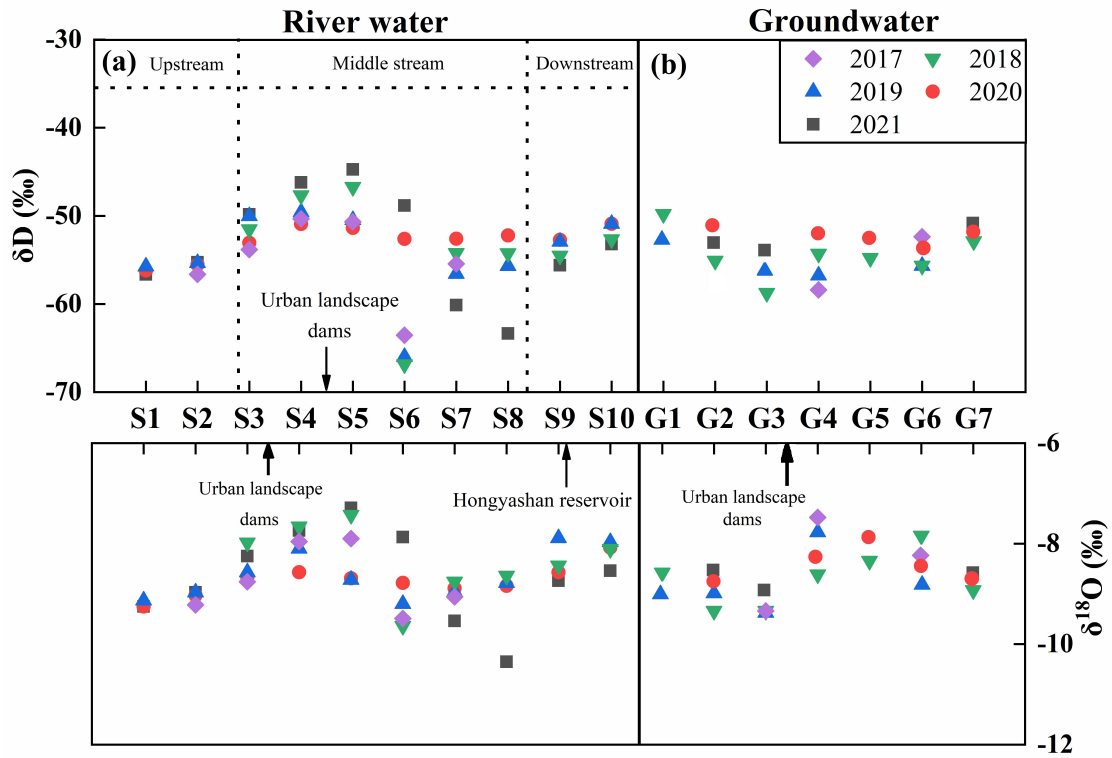
220 The amplitude of precipitation (A_{Z1}), the amplitude of the surface water outputs
221 (A_{Z2}), and the radial frequency of the annual fluctuation (c) as defined in Eq. (4) were
222 taken into consideration to estimate the mean residence time (MRT).

223 **4 Results**

224 **4.1 Spatiotemporal distribution of isotopes in different water bodies**

225 The isotopes values of the surface water in the SYR Basin show a clear
226 enrichment from upstream to downstream when viewed from space. It is worth noting
227 that landscape dams and reservoirs in urban areas alter this pattern significantly,
228 producing markedly higher isotopic compositions of surface water around such
229 structures (Fig. 2). To be more specific, the surface water throughout the entire basin
230 had average isotope values that were lower than those of the sampling points in the
231 dams region, which had values that were greater (Table 2). In addition, the dams

232 slowed the flow of the river, this resulted in isotope enrichment of the river water.
 233 Notably, these values exhibit spatial and temporal variability, with the largest δD and
 234 $\delta^{18}O$ values observed in river water, and the lowest in groundwater.



235
 236 Figure 2 Longitudinal variation of δD and $\delta^{18}O$ in river water and groundwater in the SYR Basin.

237 To be more specific, over the course of time, these values shift seasonally from
 238 spring to autumn (Table 2, Fig. 3). There was a range of values from -75.43‰ to
 239 -40.62‰ for the δD values of surface water, with an average of -53.53‰. The $\delta^{18}O$
 240 values display a varied range, from -10.43‰ to -5.53‰, with an average of -8.54‰,
 241 whereas the *d-excess* values demonstrate variability ranging from 10.26‰ to 29.72‰,
 242 with 15.28‰ as the average value. A broad spectrum of δD values are observed
 243 during the summer season, ranging from -61.27‰ to -31.16‰, with an average
 244 -48.90‰. Meanwhile, $\delta^{18}O$ values fluctuate between -9.52‰ and -3.41‰, with an
 245 average -8.12‰. The phenomenon that was observed can be traced back primarily to

246 the aftereffects of the Hongyashan Reservoir built downstream. Because the reservoir
 247 has such a large capacity for water retention, it causes significant amounts of river
 248 water to evaporate in summer, which ultimately results in a discernible enrichment of
 249 the isotopic composition. In both surface water and groundwater, δD and $\delta^{18}O$ showed
 250 significant seasonal variations (Fig. 3). Seasonal variations were more pronounced in
 251 surface water than in groundwater, with surface water showing the largest amplitude
 252 in spring and the smallest amplitude in fall, while groundwater showed closer
 253 amplitudes in all seasons, which also indicates that groundwater is less disturbed.

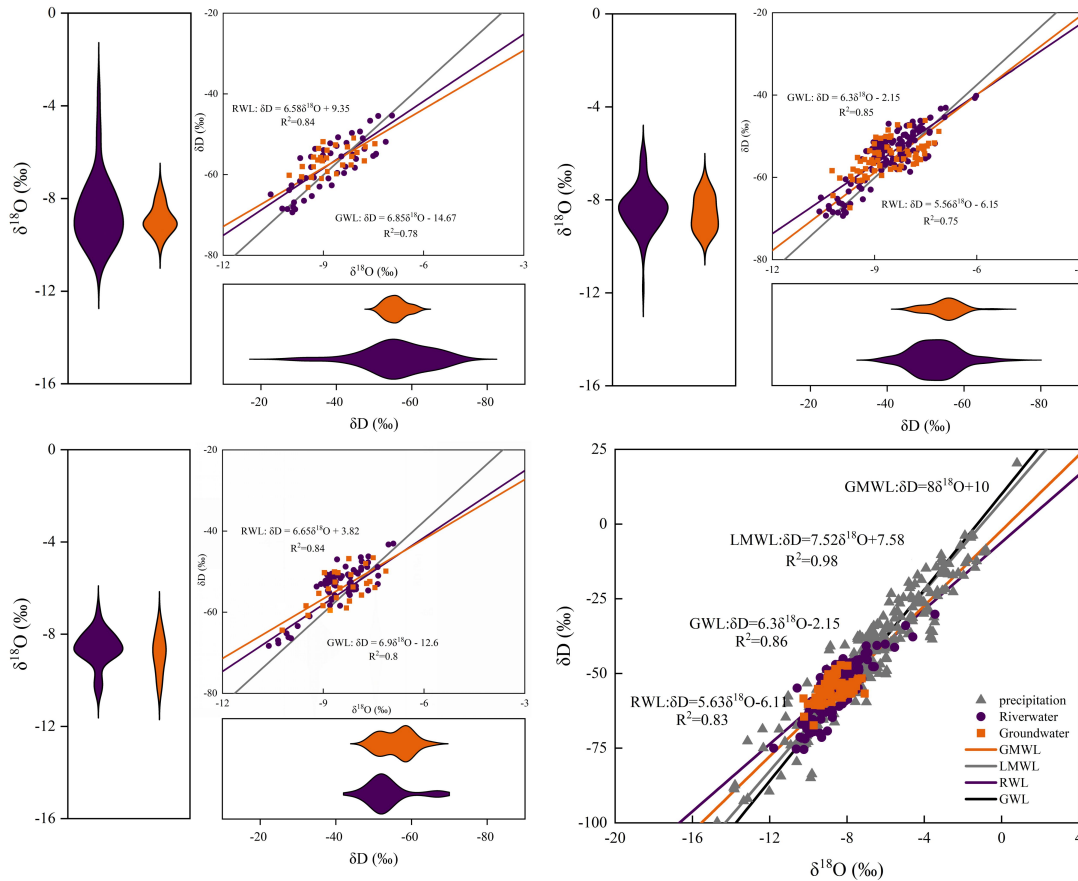
254 Table 2 Isotopic composition statistics of surface water in SYR Basin

Sampling Point	$\delta^{18}O$			δD			<i>d-excess</i>		
	Mean	Min.	Max.	Mean	Min.	Max.	Mean	Min.	Max.
S1	-9.35	-9.86	-9.06	-57.16	-59.46	-52.47	17.2	12.33	23.91
S2	-9.22	-10.02	-8.78	-56.62	-63.85	-10.02	16.46	15.53	19.28
S3	-7.74	-9.03	-7.75	-49.84	-50.76	-46.66	15.42	13.59	19.48
S4	-7.29	-8.79	-7.65	-46.22	-53.29	-46.26	14.9	11.01	18.03
S5	-7.43	-9.11	-5.53	-48.84	-56.66	-40.62	14.29	14.21	29.72
S6	-9.54	-10.43	-8.29	-60.14	-75.43	-54.40	14.31	10.26	17.62
S7	-9.04	-9.54	-8.21	-54.23	-70.04	-48.03	16.54	12.81	21.16
S8	-9.15	-10.35	-8.64	-56.37	-63.35	-52.22	16.84	14.56	19.54
S9	-8.41	-9.70	-6.02	-53.95	-65.33	-45.54	13.33	12.31	19.50
S10	-8.18	-8.84	-6.58	-51.92	-58.05	-45.39	13.48	12.21	21.72

256 4.2 The Relationship between δD and $\delta^{18}O$ values

257 As shown by the linear fitting equation $\delta D = 7.52\delta^{18}O + 7.58$, there is a significant
 258 linear positive correlation ($R^2 = 0.96$) between δD and $\delta^{18}O$ in atmospheric
 259 precipitation in the SYR Basin (Fig. 3). It is clear that the slope (7.52) and intercept
 260 (7.58) of the local meteoric water line (LMWL) are smaller than the global meteoric
 261 water line (GMWL), which can be attributed to the basin's location in an inland arid
 262 region, where precipitation disturbances are less frequent and evaporative

263 fractionation of precipitation is stronger. On the other hand, compared with the slopes
264 of the LMWL, the slopes of the surface water line (SWL) and the groundwater line
265 (GWL) are relatively close (Fig. 3), indicating that there is a strong hydraulic
266 connection between groundwater and river water in the SYR basin, and the slopes of
267 GWL and RWL show $GWL > RWL$ in all seasons, suggesting that the river water is
268 most affected by evaporation and groundwater is less affected by evaporation. In
269 addition, both surface water and groundwater sampling points were distributed near
270 the LMWL, indicating that both river water and groundwater receive recharge from
271 precipitation. Overall, the H-O isotopic composition of surface water samples from
272 the SYR showed a linear regression of $\delta D = 5.63\delta^{18}O - 6.11$, and the slope of RWL
273 was the largest in the autumn (slope = 6.65) and the smallest in the summer (slope =
274 5.56), which indicated that the river water evaporated the weakest in the autumn and
275 the strongest in the summer.



276

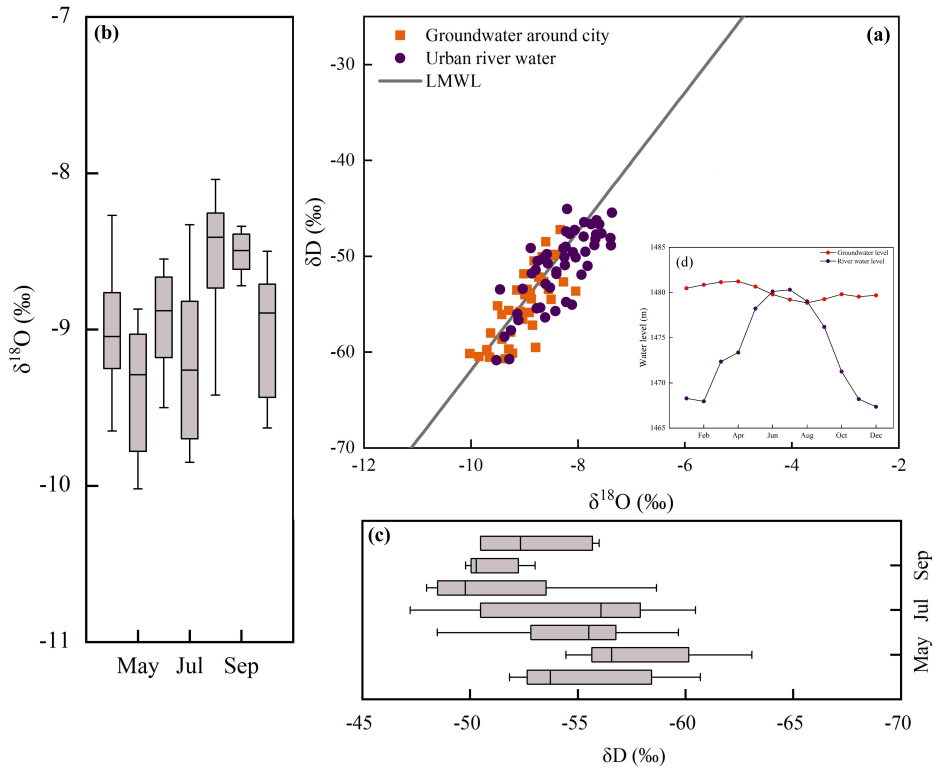
277 Figure 3 Relationship between δD and $\delta^{18}O$ in various water bodies in the SYR Basin during
 278 different seasons (a) Spring, (b) Summer, (c) Autumn, (d) The contrast between RWL, GWL,
 279 LMWL and GMWL throughout the sampling period.

280 Isotopic analysis of groundwater samples reveals a range of δD and $\delta^{18}O$ values
 281 spanning from -50.7‰ to -71.9‰ and from -7.23‰ to -10.4‰ , respectively.
 282 Moreover, the groundwater samples analyzed in the study displayed a linear
 283 regression of $\delta D = 6.3\delta^{18}O - 2.15$ ($R^2 = 0.86$). And it is interesting to note that
 284 groundwater also shows significant enrichment near the urban landscape dams (Fig.
 285 2), indicating that groundwater is also affected by evapotranspiration, mainly because
 286 the Wuwei urban area is in the region of a large alluvial fan in front of the mountains,
 287 the sand and gravel aquifers are very permeable, and the depth of groundwater burial

288 is shallow, making the groundwater more susceptible to the effects of evaporation.

289 **4.3 Impact of urbanization on groundwater**

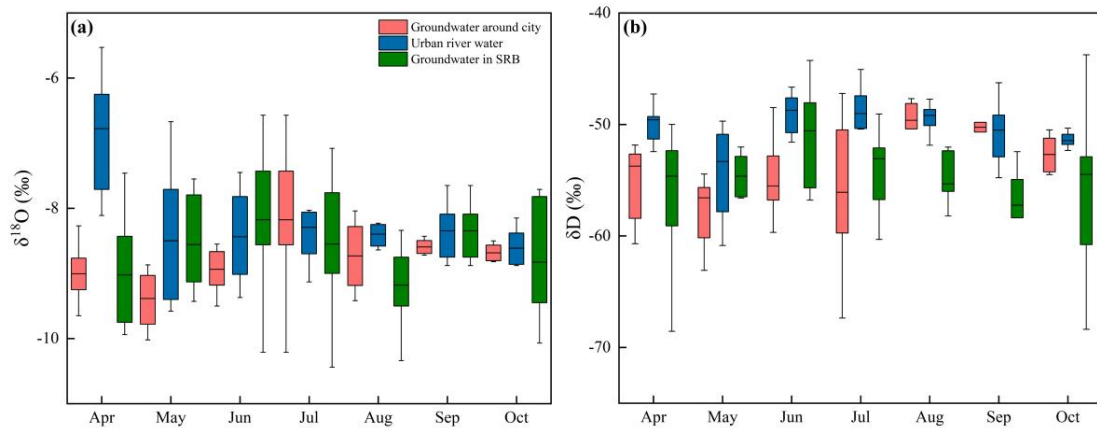
290 We compared monthly variations in isotopic values of groundwater near the city
291 with monthly variations in river water from a landscaped dam and found that the
292 monthly variations in groundwater near the city were closely related to river water
293 from a landscaped dam. The concentration of groundwater sampling sites near the city
294 near the sampling sites of the dam water indicates that the groundwater around the
295 city has similar isotopic signatures to the dam and river water (Fig. 4). This suggests
296 that groundwater near the city is recharged by river water during the summer months.
297 In addition, we demonstrated this by comparing the data of the dam river water with
298 the groundwater level. In addition, a portion of the groundwater sampling sites around
299 the city are located in the lower right corner of the LMWL, which suggests that the
300 groundwater around the city may also experience some degree of evaporation.



301
 302 Figure 4 (a) Relationship between $\delta^{18}\text{O}$ and δD of groundwater around city and urban river water;
 303 (b) Monthly variations of $\delta^{18}\text{O}$ in groundwater around city; (c) Monthly variations of δD in
 304 groundwater around city.

305 In addition, we also compared and analyzed the changes of groundwater isotope
 306 values with those of groundwater around the city in the whole basin, and found that
 307 there was a close correlation between the changes of groundwater around the city and
 308 those of the river, while the other groundwater isotope values did not have a strong
 309 correlation with the river (Fig. 5). In the urban area, the mean values of δD and $\delta^{18}\text{O}$
 310 of the dammed river water were -8.26‰ and -49.88‰ , respectively, while the mean
 311 values of δD and $\delta^{18}\text{O}$ of the groundwater around the city were -8.44‰ and -50.36‰ ,
 312 respectively, which indicated that the δD and $\delta^{18}\text{O}$ values of the groundwater around
 313 the city were similar to those of the river water in the dammed city. In addition, the
 314 isotopic mean values of δD and $\delta^{18}\text{O}$ of groundwater throughout the SYR basin were

315 -8.73‰ and -54.78‰, which are significantly different from the isotopic values of
316 river water in the urban dam.

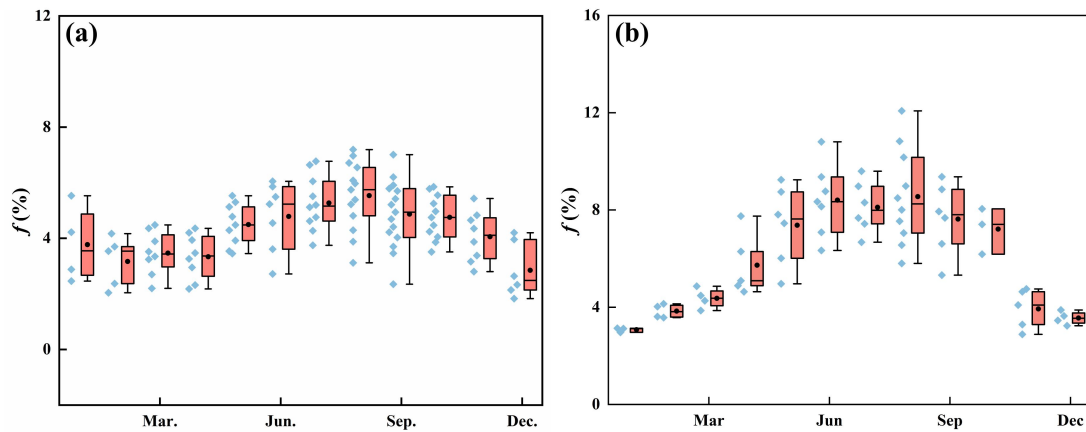


317
318 Figure 5 (a) Monthly variations of $\delta^{18}\text{O}$ in urban river water and groundwater around city, (b)
319 Monthly variations of δD in urban river water and groundwater around city.

320 4.4 Temporal and spatial variation of surface water evaporation losses in the 321 urban area of Wuwei

322 In addition to being an essential part of the hydrological cycle, evaporation is
323 widely recognized as one of the most significant factors driving climate change in
324 semi-arid regions and in telluric ecosystems (Gibson et al., 2002; Gibson and Edwards,
325 2002). An obviously spatial and temporal fluctuation can be seen in the amount of
326 surface water that is lost to evaporation in the upper mountain area as well as the
327 intermediate urban area of the SYR basin (Fig. 6). Analyzed from a time-varying
328 perspective, there is significant seasonal variation in surface water evaporation losses
329 both in the upstream mountainous region and the midstream urban area of Wuwei,
330 with the highest rates occurring during summer and the lowest during winter (Fig.6).
331 Additionally, a spatial comparison reveals that surface water evaporation losses in the
332 midstream urban area of Wuwei are significantly greater than those in the upstream

333 mountainous area.



334

335 Figure 6 Evaporation losses from surface water in different areas of the SYR (a) Upper reaches

336 mountainous area, (b) Middle reaches urban areas.

337 Differences contributing to evaporation losses from the river in the upstream and

338 midstream urban areas can be explained mainly by the landscape characteristics of the

339 basin. In the upstream of the Shiyang River, higher vegetation cover and atmospheric

340 humidity in the mountainous areas result in weaker evaporation losses, while the

341 midstream are dominated by urban land, and urban landscapes increase the watershed

342 area and slow down the river, exacerbating evaporation losses from the river.

343 5 Discussion

344 5.1 Effects of Urbanization on the Rainfall-Runoff Process

345 Fig. 7 depicts the regression model of rainfall events in the SYR Basin,

346 represented by a sine wave, and the fitting of surface water $\delta^{18}\text{O}$ across the research

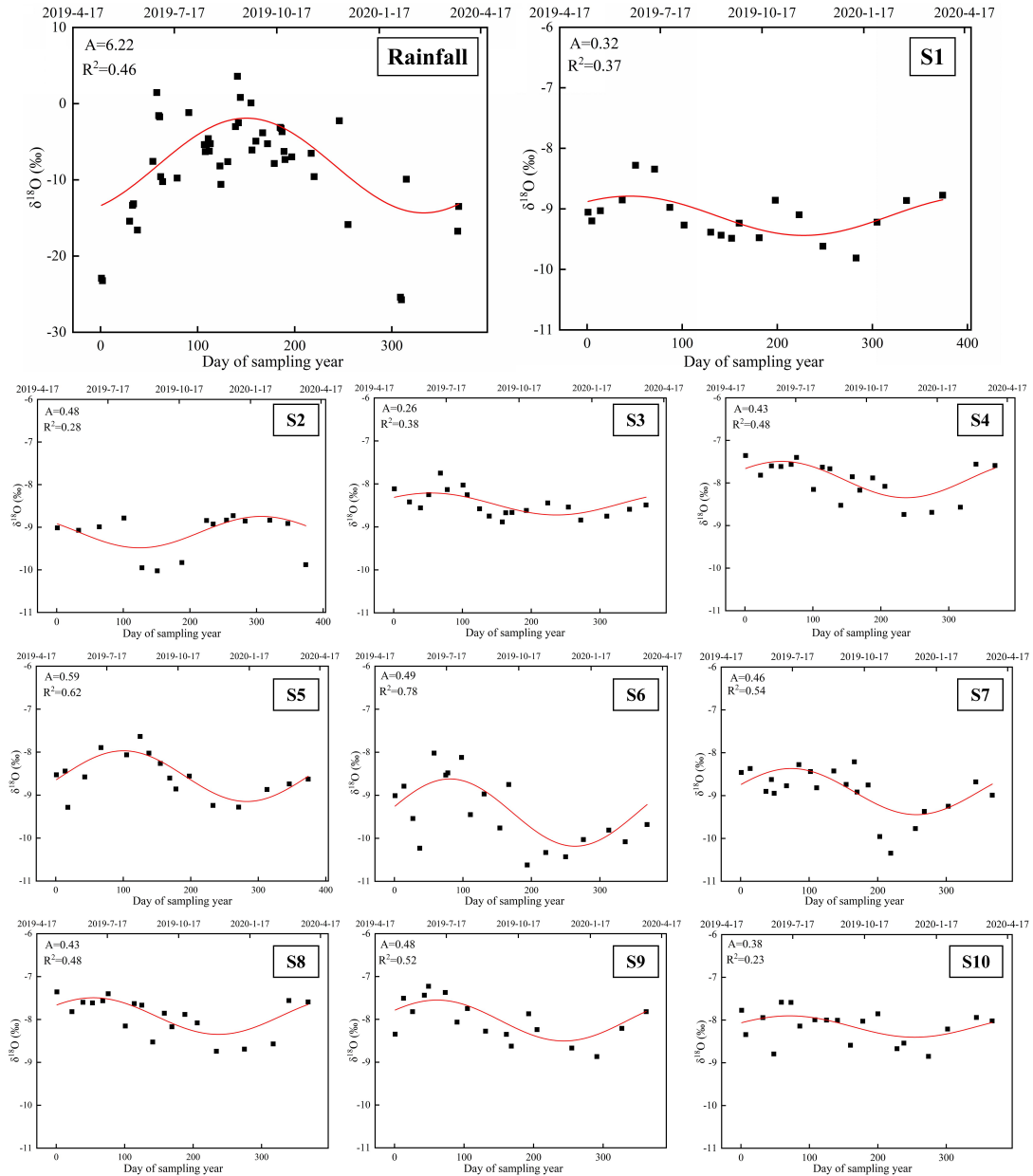
347 season. The $\delta^{18}\text{O}$ levels of precipitation reported in the SYR Basin have an excellent

348 regularity ($R^2=0.46$) and a seasonal patterns trend that effectively depicts the influence

349 of the monsoon climate on the local environment (Zhu et al., 2019). Seasonal

350 variations are seen in the generally steady $\delta^{18}\text{O}$ and $\delta^{18}\text{O}$ values of the upstream water.

351 These results indicate that the predominant component of the river water is the
352 baseflow resulting from recent precipitation runoff. Throughout the duration of the
353 study, the majority of the lowest $\delta^{18}\text{O}$ values in the 10 surface water sample points
354 were recorded during the winter, whilst the highest values were recorded during the
355 summer. These trends coincide with both the temporal variation of precipitation
356 isotopes in the SYR Basin, indicating that precipitation input is the underlying cause
357 of isotope changes in river water. Nevertheless, variations in the isotopes of river
358 water differ in range across various regions within the SYR Basin, with significant
359 variation in the degree of fit for the regression curve. The fitting degree of surface
360 water in the upper and lower reaches is relatively low ($R^2=0.37$, $R^2=0.28$, $R^2=0.23$),
361 implying limited seasonal isotopic variability in these regions. The midstream surface
362 water exhibits a notably higher degree of conformity as compared to its upstream and
363 downstream counterparts ($R^2=0.38$, $R^2=0.48$, $R^2=0.62$, $R^2=0.78$, $R^2=0.54$, $R^2=0.48$,
364 $R^2=0.52$). Moreover, the isotopic composition of surface water throughout this area
365 exhibits notable cyclic variations.



366

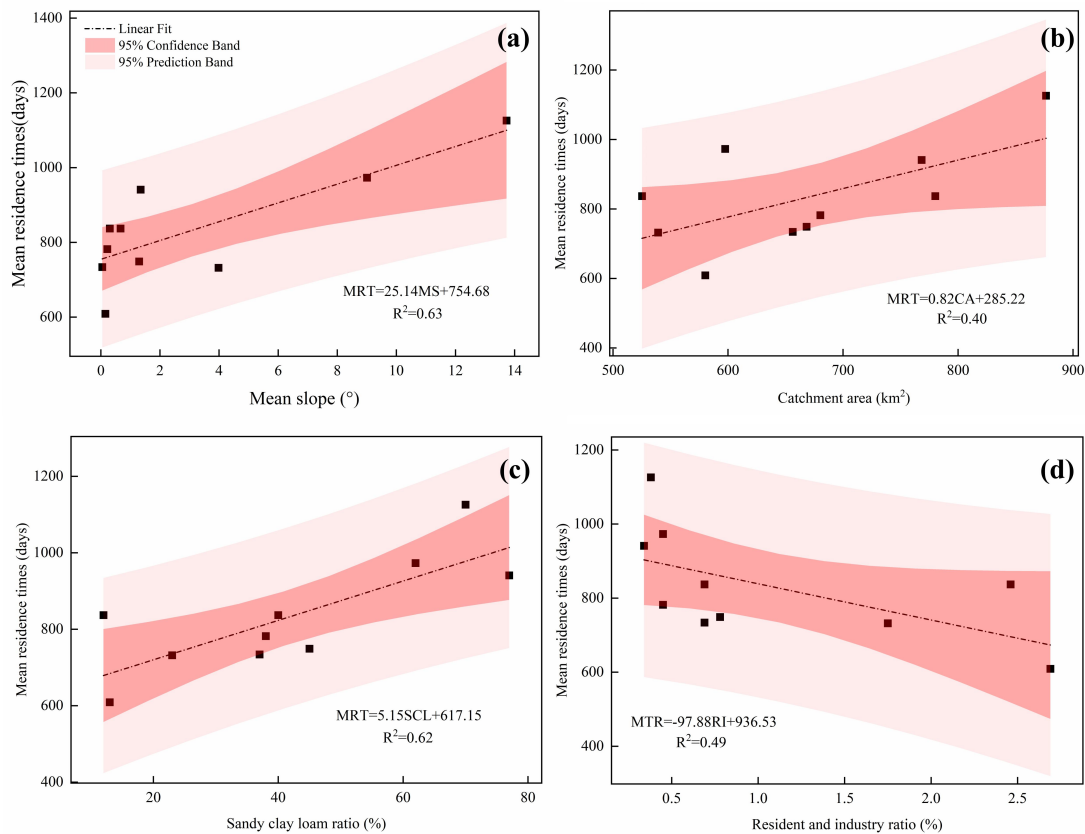
367 Figure 7 Fits the annual regression model of $\delta^{18}\text{O}$ in SYR Basin precipitation and river water (time:
 368 2019/4/17—2020/4/23; S1-S10 are surface water sampling points).

369 The reasons for differences in isotope periodicity in different regions may be
 370 attributed to local water management systems, topographic features and urban
 371 development. At points S1, S2, and S10, the correlation of model simulations was low,
 372 which could be attributed to the presence of Xiyang Reservoir in the upstream as well
 373 as Hongyashan Reservoir in the downstream (Sang et al., 2023), where seasonal

374 variations in the isotope values of the river water are interfered by the reservoir
375 dispatching activities. At points S3 to S5, the correlation of the model simulation is
376 higher, which is because in the middle reaches of the SYR basin, the expansion of
377 urban built-up areas leads to a significant increase in surface runoff during the rainy
378 season, and according to the land use data, the land area of the towns in Wuwei City
379 has continued to increase by 134.38 km² from 2010 to 2018, resulting in the surface
380 water showing a cyclical trend comparable to that of the precipitation. Since the 1950s,
381 in order to better utilize water resources, 13 small and medium-sized reservoirs with a
382 total storage capacity of 900,000 m³ were constructed during this period (Ma et al.,
383 2010), increasing the proportion of rainfall in the runoff constituents as a result of The
384 correlation of the model simulation is at a high level at points S6~S9, where, in
385 contrast to the high-elevation areas in the upper reaches, the terrain in the middle and
386 lower reaches of the SYR basin is relatively flat, mainly with cultivated land and
387 deserts, and is less disturbed by human activities (Sun et al., 2021), which further
388 reflects the responsiveness to recent precipitation inputs.

389 The Dunnett's test revealed a significant difference ($P < 0.05$) between the MRT
390 of the river and the annual magnitude of $\delta^{18}\text{O}$ of the river. We further investigated the
391 relationship between the estimated mean residence time and basin landscape features
392 such as topography (Fig. 8). Using the digital elevation model (DEM) to calculate the
393 mean slope of the SYR basin, we found that the mean residence time was also
394 strongly correlated with the mean basin slope ($R^2 = 0.63$), and that the upper reaches
395 of the Shiyang River basin are mainly high-elevation mountainous areas, where the

396 topography is sloped, but where the vegetation cover is high and dominated by alpine
 397 meadows, subalpine scrub and Qinghai spruce (Zhang et al. 2023), the greater slope
 398 leads to a higher gravitational potential, which tends to result in a negative correlation
 399 with mean residence time (McGuire et al., 2005), which also contributes to the
 400 potentially higher MRT values in the upstream mountains. In our study, catchment
 401 area (CA) had a low correlation with MRT ($R^2 = 0.40$), and a weak relationship
 402 between catchment area and MRT has been observed in other studies (McGlynn et al.,
 403 2003; McGuire et al., 2005).



404
 405 **Figure 8** Correlation between mean slope of the basin (a), catchment area (b), sand clay loam ratio
 406 (c), ratio of residential and industrial areas to total basin area (d) and MRT.

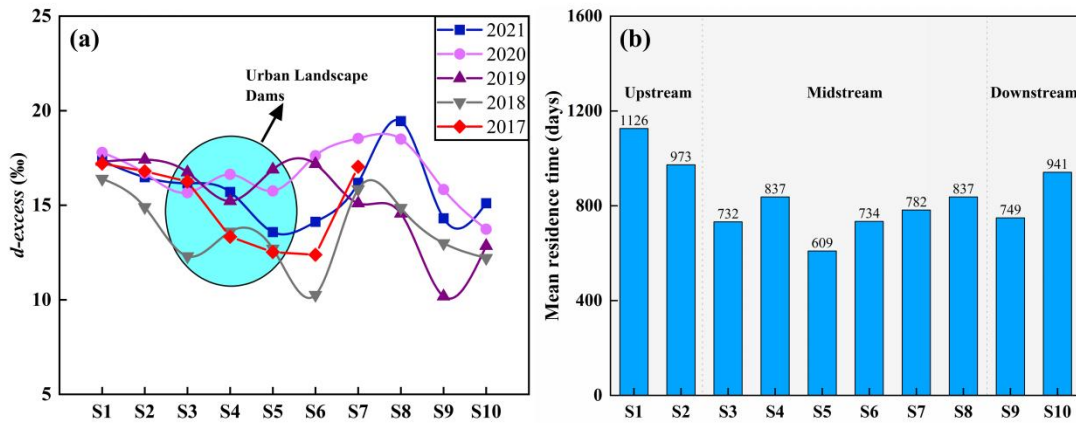
407 Soil is an important component of basin hydrology, and the physical properties
 408 of soil, such as water-holding capacity and pore space distribution, have an important

409 influence on the response to precipitation in the basin and the sand-clay-loam soil
410 ratio is used here to investigate the possible relationship with MRT. The results
411 showed that the content of sand clay loam ratio showed a strong positive correlation
412 with MRT ($R^2=0.62$). Wuwei City is located in the pre-mountain flood-fan belt, and
413 the soil is dominated by sandy soil (Zhang et al., 2023), which is loose in texture, has
414 good permeability and good water retention properties, and is mainly used for
415 agricultural cultivation. Its good permeability increases the vertical movement of
416 water and the length of flow paths, leading to a longer MRT. There is a strong
417 negative correlation between the MRT and the ratios of resident and industrial areas
418 (RI) ($R^2=0.49$), which also indicates that as urbanization progresses, with the increase
419 of urban land, this undoubtedly leads to a significant shortening of the MRT. However,
420 the MRT in the mid-river urban area is not much shorter as compared to the
421 downstream, which may be attributed to the fact that the mid-river The large number
422 of landscape dams constructed in the urban areas, currently 51 urban landscape dams
423 have been built in the peri-urban areas of Wuwei City, and the considerable number of
424 landscape dams may have counteracted the impact of the urban land use, resulting in a
425 lengthening of the MRT in the middle reaches as well.

426 **5.2 Effects of Water Conservancy Projects in Urban Areas on Isotope Dynamics**

427 Recent studies have suggested that the development of dam-reservoir systems
428 may result in river fragmentation and modifications in flow regimes in terms of their
429 volume, frequency, and duration (Négrel et al., 2016; Murgulet et al., 2016; Peñas and
430 Barquín, 2019; Maavara et al., 2020). Furthermore, chemical-containing nutrient

431 migration, such as phosphorus, may occur during sediment movement, resulting in
432 widespread eutrophication problems (Yang et al., 2007; Duan et al., 2019). As of 2019,
433 a total of 51 urban landscape dams, primarily consisting of artificial landscape
434 waterfalls and rubber dams, have been constructed in and around Wuwei city (Zhu et
435 al., 2021). In the metropolitan coast of Wuwei, many landscape dams have led to
436 isotopic enrichment in surface water. This damping effect has been observed in
437 numerous dammed rivers across the globe, including the Rio Grande in the
438 southwestern United States (Vitvar et al., 2007) and the Ebro River in Spain (Négre
439 et al., 2016), as evidenced by isotopic tracers. In the metropolitan coast of Wuwei, a
440 number of landscape dams have led to the enrichment of isotopic tracers in the surface
441 water. The results indicate that the δD and $\delta^{18}O$ levels of the surface water at the
442 outflow of Wuwei City are greater than those at the inflow (Fig. 2). Moreover, the
443 influence of evaporation on isotopic composition should not be overlooked, as it can
444 lead to a decrease in *d-excess* values (Peng et al., 2012). Consistent with previous
445 studies (Wang et al., 2019), we observed that the *d-excess* of influent water was higher
446 than that of urban river water. This observation further supports the accumulation of
447 heavy H-O isotopes in the surface waters of the dam areas, as shown in Fig. 6a. In
448 contrast, due to the confluence of tributaries prior to the S7 sampling point, the river
449 water has lower isotopic values, resulting in elevated *d-excess* values between S6 and
450 S8.



451

452 Figure 9 (a) The longitudinal variation of the surface water *d-excess* of the SYR, (b) The

453 longitudinal variation of the surface water MRT of the SYR.

454 5.3 Effects of Urbanization on the Water Cycle of basins

455 Localized microclimates in urban areas allow for changes in precipitation and

456 evapotranspiration processes, while urbanization alters the pristine subsurface,

457 complicating water cycle processes in the basin (Jacobson, 2011; Westra et al., 2014;

458 Oudin et al., 2018). In terms of the impact on runoff, it is mainly reflected in the

459 increase of surface impermeability due to urbanization, the land use area of Wuwei

460 urban land increased by about 134.38 km² from 2010 to 2018, which greatly

461 weakened the infiltration process in urban areas, and the rainfall runoff process

462 simulated by sinusoidal cyclic regression method showed that there were significant

463 differences in the river metro in different parts of the Shiyang River Basin, and that

464 the middle reaches of the river had the highest degree of urbanization, and the time of

465 the metro was the shortest, which further increases the contribution of rainfall to

466 runoff. Regarding the effect of urbanization on evapotranspiration, a large number of

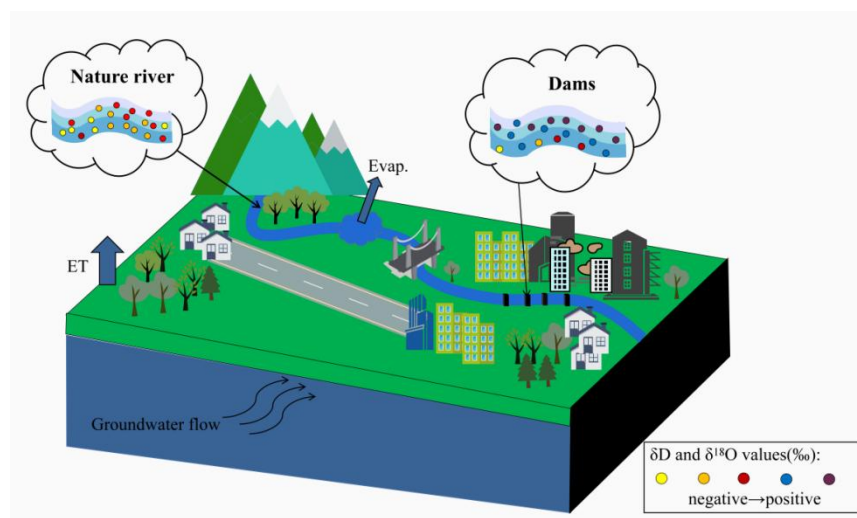
467 dams were constructed on the Shiyang River and flowed through the urban area of

468 Wuwei, causing significant evapotranspiration losses, in addition, these landscape

469 dams also led to hydrogen and oxygen isotope enrichment (Fig. 10), and the
470 numerous reservoirs that were constructed for the construction and development of
471 the city (Ma et al., 2010), and these reservoirs also contributed to a significant
472 evapotranspiration loss effect, which has been previously confirmed in our study was
473 also confirmed (Sang et al., 2023). On the other hand, our study found that the
474 isotopic compositions and trends of urban nearshore groundwater were similar to
475 those of surface water, which suggests that there is a close correlation between urban
476 nearshore groundwater and river water, and that the difference in water levels between
477 river water and groundwater may be the main reason for river recharge of urban
478 nearshore groundwater (Fig. 4). In the rainy season, the river level gradually rises,
479 which decreases the difference between the water levels of urban nearshore
480 groundwater and river water, and the river water recharges the groundwater, and in the
481 dry season, the river level decreases, and the urban nearshore groundwater, which is
482 buried at a shallow depth, in turn recharges the river.

483 In addition, the growth of urbanization has had a dramatic impact on the water
484 environment in cities, where water problems occur frequently (Giri and Qiu, 2016;
485 Ma et al., 2022). Urbanization has increased impervious surfaces such as parking lots,
486 rooftops, roads, and sidewalks, leading to increased runoff, which creates additional
487 pathways for pollutants to be transported from landscapes to water bodies (Ren et al.,
488 2014; Wilson and Weng, 2010; Nolan et al., 2023). On the other hand, agricultural
489 activities have increased some of the fertilizers, pesticides, herbicides and dairy
490 manure in the farmland into the nearest water bodies, which can directly and

491 indirectly affect will reduce water quality (Yu et al., 2013). The Shiyang River Basin
492 in the Northwest Arid Zone is an inland river basin with the highest development
493 intensity and the sharpest conflict between water supply and demand in the region.
494 The Liangzhou district in the central part of the Shiyang River basin is the most
495 densely populated artificial oasis with the largest scale of water demand in the entire
496 basin. Our previous study found that direct discharge of industrial and community
497 domestic wastewater into the river led to deterioration of surface water quality around
498 the Shiyang River basin (Ma et al., 2021). In addition agricultural activities have less
499 impact on the upper reaches of the Shiyang River and relatively more impact on the
500 middle and lower reaches , and the application of nitrogen-based fertilizers during
501 agricultural cultivation is the main cause of high NH_4^+ and NO_3^- concentrations in the
502 area (Ma et al., 2021), which may also lead to increased salinity and accelerated
503 eutrophication of the river, threatening the safety of the basin's water environment.
504 Overall, human activities (urbanization) may alter the water cycle processes inherent
505 in inland river basins, and the implications of such changes need to be further
506 explored.



508 Figure 10 Schematic diagram of the effect of urbanization on river isotope dynamics.

509 **6 Conclusions**

510 In this study, we investigated the hydrometeorological and isotopic data of the
511 Shiyang River Basin from 2017 to 2021, and our investigations showed that
512 urbanization had a significant impact on the water cycle of the basin. The results
513 showed that the isotopic values of the river water showed a significant enrichment
514 from upstream to downstream, but facilities such as landscape dams and reservoirs in
515 the urban area significantly altered this natural pattern, and the isotopic values of the
516 river water in the urban area ($\delta D = -48.31\text{‰}$; $\delta^{18}O = -7.49\text{‰}$) were higher than those of
517 the natural river water ($\delta D = -55.77\text{‰}$; $\delta^{18}O = -8.98\text{‰}$), and landscape dams aggravated
518 the evaporation losses of river water, due to the increase of urban land area, which
519 accelerated the rainfall-runoff conversion process, the residence time of surface water
520 in different regions of the Shiyang River Basin had obvious differences, and the MRT
521 from the upstream to the downstream showed a fluctuating downward process, which
522 was shortened from 1,126 days in the upstream to 941 days in the downstream, and
523 the MRT was mainly controlled by the basin's landscape features. In addition, there
524 was a strong relationship between the isotopic composition of the reservoir and the
525 surrounding groundwater. Overall, urbanization has a profound impact on the
526 hydrological system of the basin, and the results of this study can provide some
527 references for future research on urbanization and the water cycle, and improve our
528 understanding of the hydrological processes of basin in arid zones.

529 **Acknowledgements**

530 This research was financially supported by the National Natural Science
531 Foundation of China (41971036, 41867030).

532 **Data availability Statement**

533 The isotopic data that support the findings of this study are openly available in
534 Zhu, Guofeng (2022), “Stable water isotope monitoring network of different water
535 bodies in SYR Basin, a typical arid river in China”, Mendeley Data, V1, doi:
536 10.17632/vhm44t74sy.1. The source of soil data comes from the Harmonized World
537 Soil Database (HWSD) constructed by the Food and Agriculture Organization of the
538 United Nations (FAO) and the International Institute for Applied Systems (IIASA) on
539 2009. The land-use and land-cover change data of the Shiyang River Basin were
540 obtained from Chinese Academy of Sciences, the data centre of resources and
541 environmental science (<http://www.resdc.cn>).

542 **Competing Interests**

543 We undersigned declare that this manuscript entitled “Effects of Urbanization on
544 the water cycle in the SYR Basin: Based on stable isotope method” is original, has not
545 been published before and is not currently being considered for publication elsewhere.

546 The authors declare that they have no known competing financial interests or
547 personal relationships that could have appeared to influence the work reported in this
548 paper.

549 **Reference**

550 **Anderson, B. J., Slater, L. J., Dadson, S. J., Blum, A. G., and Prosdocimi, I.:**
551 **Statistical Attribution of the Influence of Urban and Tree Cover Change on**
552 **Streamflow: A Comparison of Large Sample Statistical Approaches, Water**

553 Resources Research, 58, e2021WR030742,
554 <https://doi.org/10.1029/2021WR030742>, 2022.

555 Asano, Y., Uchida, T., and Ohte, N.: Residence times and flow paths of water in steep
556 unchannelled catchments, Tanakami, Japan, *Journal of Hydrology*, 261, 173–192,
557 [https://doi.org/10.1016/S0022-1694\(02\)00005-7](https://doi.org/10.1016/S0022-1694(02)00005-7), 2002.

558 Baker, A.: Land Use and Water Quality, in: *Encyclopedia of Hydrological Sciences*,
559 edited by: Anderson, M. G. and McDonnell, J. J., John Wiley & Sons, Ltd,
560 Chichester, UK, hsa195, <https://doi.org/10.1002/0470848944.hsa195>, 2005.

561 Bhaskar, A. S. and Welty, C.: Analysis of subsurface storage and streamflow
562 generation in urban basins, *Water Resour. Res.*, 51, 1493–1513,
563 <https://doi.org/10.1002/2014WR015607>, 2015.

564 Blum, A. G., Ferraro, P. J., Archfield, S. A., and Ryberg, K. R.: Causal Effect of
565 Impervious Cover on Annual Flood Magnitude for the United States,
566 *Geophysical Research Letters*, 47, e2019GL086480,
567 <https://doi.org/10.1029/2019GL086480>, 2020.

568 Bruwier, M., Maravat, C., Mustafa, A., Teller, J., Piroton, M., Erpicum, S.,
569 Archangeau, P., and Dewals, B.: Influence of urban forms on surface flow in
570 urban pluvial flooding, *Journal of Hydrology*, 582, 124493,
571 <https://doi.org/10.1016/j.jhydrol.2019.124493>, 2020.

572 Burian, S. J. and Shepherd, J. M.: Effect of urbanization on the diurnal rainfall pattern
573 in Houston, *Hydrol. Process.*, 19, 1089–1103, <https://doi.org/10.1002/hyp.5647>,
574 2005.

575 Caldwell, P. V., Sun, G., McNulty, S. G., Cohen, E. C., and Moore Myers, J. A.:
576 Impacts of impervious cover, water withdrawals, and climate change on river
577 flows in the conterminous US, *Hydrol. Earth Syst. Sci.*, 16, 2839–2857,
578 <https://doi.org/10.5194/hess-16-2839-2012>, 2012.

579 Chen, G., Li, X., Liu, X., Chen, Y., Liang, X., Leng, J., Xu, X., Liao, W., Qiu, Y., Wu,
580 Q., and Huang, K.: Global projections of future urban land expansion under
581 shared socioeconomic pathways, *Nat Commun*, 11, 537,
582 <https://doi.org/10.1038/s41467-020-14386-x>, 2020.

583 Dansgaard, W.: Stable isotopes in precipitation, *Tellus*, 16, 436–468,
584 <https://doi.org/10.1111/j.2153-3490.1964.tb00181.x>, 1964.

585 De Niel, J. and Willems, P.: Climate or land cover variations: what is driving observed
586 changes in river peak flows? A data-based attribution study, *Hydrol. Earth Syst.*
587 *Sci.*, 23, 871–882, <https://doi.org/10.5194/hess-23-871-2019>, 2019.

588 Deng, K., Yang, S., Lian, E., Li, C., Yang, C., and Wei, H.: Three Gorges Dam alters
589 the Changjiang (Yangtze) river water cycle in the dry seasons: Evidence from
590 H-O isotopes, *Science of The Total Environment*, 562, 89–97,
591 <https://doi.org/10.1016/j.scitotenv.2016.03.213>, 2016.

592 Duan, W., Hanasaki, N., Shiogama, H., Chen, Y., Zou, S., Nover, D., Zhou, B., and
593 Wang, Y.: Evaluation and Future Projection of Chinese Precipitation Extremes
594 Using Large Ensemble High-Resolution Climate Simulations, *Journal of Climate*,
595 32, 2169–2183, <https://doi.org/10.1175/JCLI-D-18-0465.1>, 2019.

596 Fekete, B. M., Gibson, J. J., Aggarwal, P., and Vörösmarty, C. J.: Application of
597 isotope tracers in continental scale hydrological modeling, *Journal of Hydrology*,
598 330, 444–456, <https://doi.org/10.1016/j.jhydrol.2006.04.029>, 2006.

599 Flörke, M., Schneider, C., and McDonald, R. I.: Water competition between cities and
600 agriculture driven by climate change and urban growth, *Nat Sustain*, 1, 51–58,
601 <https://doi.org/10.1038/s41893-017-0006-8>, 2018.

602 Förstel, H. and Hütten, H.: Oxygen isotope ratios in German groundwater, *Nature*,
603 304, 614–616, <https://doi.org/10.1038/304614a0>, 1983.

604 Fu, X., Yang, X., and Sun, X.: Spatial and Diurnal Variations of Summer Hourly
605 Rainfall Over Three Super City Clusters in Eastern China and Their Possible
606 Link to the Urbanization, *JGR Atmospheres*, 124, 5445–5462,
607 <https://doi.org/10.1029/2019JD030474>, 2019.

608 Gammons, C. H., Poulson, S. R., Pellicori, D. A., Reed, P. J., Roesler, A. J., and
609 Petrescu, E. M.: The hydrogen and oxygen isotopic composition of precipitation,
610 evaporated mine water, and river water in Montana, USA, *Journal of Hydrology*,
611 328, 319–330, <https://doi.org/10.1016/j.jhydrol.2005.12.005>, 2006.

612 Gessner, M. O., Hinkelmann, R., Nützmann, G., Jekel, M., Singer, G., Lewandowski,
613 J., Nehls, T., and Barjenbruch, M.: Urban water interfaces, *Journal of Hydrology*,
614 514, 226–232, <https://doi.org/10.1016/j.jhydrol.2014.04.021>, 2014.

615 Gibson, J. J., Edwards, T. W. D., Birks, S. J., St Amour, N. A., Buhay, W. M.,
616 McEachern, P., Wolfe, B. B., and Peters, D. L.: Progress in isotope tracer

617 hydrology in Canada, *Hydrol. Process.*, 19, 303–327,
618 <https://doi.org/10.1002/hyp.5766>, 2005.

619 Gibson, J. J. and Edwards, T. W. D.: Regional water balance trends and
620 evaporation-transpiration partitioning from a stable isotope survey of lakes in
621 northern Canada: REGIONAL WATER BALANCE USING STABLE
622 ISOTOPES, *Global Biogeochem. Cycles*, 16, 10-1-10–14,
623 <https://doi.org/10.1029/2001GB001839>, 2002.

624 Gibson, J. J., Prepas, E. E., and McEachern, P.: Quantitative comparison of lake
625 throughflow, residency, and catchment runoff using stable isotopes: modelling
626 and results from a regional survey of Boreal lakes, *Journal of Hydrology*, 2002.

627 Gillefalk, M., Tetzlaff, D., Hinkelmann, R., Kuhlemann, L.-M., Smith, A., Meier, F.,
628 Maneta, M. P., and Soulsby, C.: Quantifying the effects of urban green space on
629 water partitioning and ages using an isotope-based ecohydrological model,
630 *Hydrol. Earth Syst. Sci.*, 25, 3635–3652,
631 <https://doi.org/10.5194/hess-25-3635-2021>, 2021.

632 Giri, S. and Qiu, Z.: Understanding the relationship of land uses and water quality in
633 Twenty First Century: A review, *Journal of Environmental Management*, 173,
634 41–48, <https://doi.org/10.1016/j.jenvman.2016.02.029>, 2016.

635 Grimm, N. B., Faeth, S. H., Golubiewski, N. E., Redman, C. L., Wu, J., Bai, X., and
636 Briggs, J. M.: Global Change and the Ecology of Cities, *Science*, 319, 756–760,
637 <https://doi.org/10.1126/science.1150195>, 2008.

638 Guan, M., Sillanpää, N., and Koivusalo, H.: Storm runoff response to rainfall pattern,
639 magnitude and urbanization in a developing urban catchment: Storm Runoff
640 Response to Rainfall Pattern, Magnitude and Urbanization, *Hydrol. Process.*,
641 n/a-n/a, <https://doi.org/10.1002/hyp.10624>, 2015.

642 Hamilton, S. K., Bunn, S. E., Thoms, M. C., and Marshall, J. C.: Persistence of
643 aquatic refugia between flow pulses in a dryland river system(Cooper Creek,
644 Australia), *Limnol. Oceanogr.*, 50, 743–754,
645 <https://doi.org/10.4319/lo.2005.50.3.0743>, 2005.

646 Han, S., Slater, L., Wilby, R. L., and Faulkner, D.: Contribution of urbanisation to
647 non-stationary river flow in the UK, *Journal of Hydrology*, 613, 128417,
648 <https://doi.org/10.1016/j.jhydrol.2022.128417>, 2022.

649 Jacobson, C. R.: Identification and quantification of the hydrological impacts of
650 imperviousness in urban catchments: A review, *Journal of Environmental*
651 *Management*, 92, 1438–1448, <https://doi.org/10.1016/j.jenvman.2011.01.018>,
652 2011.

653 Liu, J., Shen, Z., and Chen, L.: Assessing how spatial variations of land use pattern
654 affect water quality across a typical urbanized basin in Beijing, China,
655 *Landscape and Urban Planning*, 176, 51–63,
656 <https://doi.org/10.1016/j.landurbplan.2018.04.006>, 2018.

657 Ma, H., Zhu, G., Zhang, Y., Sang, L., Wan, Q., Zhang, Z., Xu, Y., and Qiu, D.: Ion
658 migration process and influencing factors in inland river basin of arid area in

659 China: a case study of Shiyang River Basin, *Environ Sci Pollut Res*, 28,
660 56305–56318, <https://doi.org/10.1007/s11356-021-14484-3>, 2021.

661 Ma, J., Pan, F., Chen, L., Edmunds, W. M., Ding, Z., He, J., Zhou, K., and Huang, T.:
662 Isotopic and geochemical evidence of recharge sources and water quality in the
663 Quaternary aquifer beneath Jinchang city, NW China, *Applied Geochemistry*, 25,
664 996–1007, <https://doi.org/10.1016/j.apgeochem.2010.04.006>, 2010.

665 Ma, X., Li, N., Yang, H., and Li, Y.: Exploring the relationship between urbanization
666 and water environment based on coupling analysis in Nanjing, East China,
667 *Environ Sci Pollut Res*, 29, 4654–4667,
668 <https://doi.org/10.1007/s11356-021-15161-1>, 2022.

669 Maavara, T., Chen, Q., Van Meter, K., Brown, L. E., Zhang, J., Ni, J., and Zarfl, C.:
670 River dam impacts on biogeochemical cycling, *Nat Rev Earth Environ*, 1,
671 103–116, <https://doi.org/10.1038/s43017-019-0019-0>, 2020.

672 Małoszewski, P., Rauert, W., Stichler, W., and Herrmann, A.: Application of flow
673 models in an alpine catchment area using tritium and deuterium data, *Journal of*
674 *Hydrology*, 66, 319–330, [https://doi.org/10.1016/0022-1694\(83\)90193-2](https://doi.org/10.1016/0022-1694(83)90193-2), 1983.

675 Martin, K. L., Hwang, T., Vose, J. M., Coulston, J. W., Wear, D. N., Miles, B., and
676 Band, L. E.: basin impacts of climate and land use changes depend on magnitude
677 and land use context, *Ecohydrology*, 10, e1870, <https://doi.org/10.1002/eco.1870>,
678 2017.

679 McDonough, L. K., Santos, I. R., Andersen, M. S., O’Carroll, D. M., Rutledge, H.,
680 Meredith, K., Oudone, P., Bridgeman, J., Gooddy, D. C., Sorensen, J. P. R.,

681 Lapworth, D. J., MacDonald, A. M., Ward, J., and Baker, A.: Changes in global
682 groundwater organic carbon driven by climate change and urbanization, *Nat*
683 *Commun*, 11, 1279, <https://doi.org/10.1038/s41467-020-14946-1>, 2020.

684 McGlynn, B., McDonnell, J., Stewart, M., and Seibert, J.: On the relationships
685 between catchment scale and streamwater mean residence time, *Hydrol. Process.*,
686 17, 175–181, <https://doi.org/10.1002/hyp.5085>, 2003.

687 McGuire, K. J., McDonnell, J. J., Weiler, M., Kendall, C., McGlynn, B. L., Welker, J.
688 M., and Seibert, J.: The role of topography on catchment-scale water residence
689 time: CATCHMENT-SCALE WATER RESIDENCE TIME, *Water Resour. Res.*,
690 41, <https://doi.org/10.1029/2004WR003657>, 2005.

691 Murgulet, D., Murgulet, V., Spalt, N., Douglas, A., and Hay, R. G.: Impact of
692 hydrological alterations on river-groundwater exchange and water quality in a
693 semi-arid area: Nueces River, Texas, *Science of The Total Environment*, 572,
694 595–607, <https://doi.org/10.1016/j.scitotenv.2016.07.198>, 2016.

695 Négrel, P., Petelet-Giraud, E., and Millot, R.: Tracing water cycle in regulated basin
696 using stable $\delta^{18}\text{O}$ – $\delta^2\text{H}$ isotopes: The Ebro river basin (Spain), *Chemical Geology*,
697 422, 71–81, <https://doi.org/10.1016/j.chemgeo.2015.12.009>, 2016.

698 Nolan, T. M., Reynolds, L. J., Sala-Comorera, L., Martin, N. A., Stephens, J. H.,
699 O'Hare, G. M. P., O'Sullivan, J. J., and Meijer, W. G.: Land use as a critical
700 determinant of faecal and antimicrobial resistance gene pollution in riverine
701 systems, *Science of The Total Environment*, 871, 162052,
702 <https://doi.org/10.1016/j.scitotenv.2023.162052>, 2023.

703 Oudin, L., Salavati, B., Furusho-Percot, C., Ribstein, P., and Saadi, M.: Hydrological
704 impacts of urbanization at the catchment scale, *Journal of Hydrology*, 559,
705 774–786, <https://doi.org/10.1016/j.jhydrol.2018.02.064>, 2018.

706 Peñas, F. J. and Barquín, J.: Assessment of large-scale patterns of hydrological
707 alteration caused by dams, *Journal of Hydrology*, 572, 706–718,
708 <https://doi.org/10.1016/j.jhydrol.2019.03.056>, 2019.

709 Peng, T.-R., Huang, C.-C., Wang, C.-H., Liu, T.-K., Lu, W.-C., and Chen, K.-Y.:
710 Using oxygen, hydrogen, and tritium isotopes to assess pond water's contribution
711 to groundwater and local precipitation in the pediment tableland areas of
712 northwestern Taiwan, *Journal of Hydrology*, 450–451, 105–116,
713 <https://doi.org/10.1016/j.jhydrol.2012.05.021>, 2012.

714 Pickett, S. T. A., Cadenasso, M. L., Grove, J. M., Boone, C. G., Groffman, P. M.,
715 Irwin, E., Kaushal, S. S., Marshall, V., McGrath, B. P., Nilon, C. H., Pouyat, R.
716 V., Szlavecz, K., Troy, A., and Warren, P.: Urban ecological systems: Scientific
717 foundations and a decade of progress, *Journal of Environmental Management*, 92,
718 331–362, <https://doi.org/10.1016/j.jenvman.2010.08.022>, 2011.

719 Qian, H., Dou, Y., Li, X.J., Yang, B.C., and Zhao, Z.H.: Changes of $\delta^{18}\text{O}$ and δD
720 along Dousitu River and its indication of river water evaporation. *Hydrogeol.*
721 *Eng. Geol.* 34 (1), 107–112,
722 <https://doi.org/10.16030/j.cnki.issn.1000-3665.2007.01.024>, 2007.

723 Ren, L., Cui, E., and Sun, H.: Temporal and spatial variations in the relationship
724 between urbanization and water quality, *Environ Sci Pollut Res*, 21,
725 13646–13655, <https://doi.org/10.1007/s11356-014-3242-8>, 2014.

726 Rodgers, P., Soulsby, C., Waldron, S., and Tetzlaff, D.: Using stable isotope tracers to
727 assess hydrological flow paths, residence times and landscape influences in a
728 nested mesoscale catchment, *Hydrol. Earth Syst. Sci.*, 9, 139–155,
729 <https://doi.org/10.5194/hess-9-139-2005>, 2005.

730 Salvadore, E., Bronders, J., and Batelaan, O.: Hydrological modelling of urbanized
731 catchments: A review and future directions, *Journal of Hydrology*, 529, 62–81,
732 <https://doi.org/10.1016/j.jhydrol.2015.06.028>, 2015.

733 Sang, L., Zhu, G., Xu, Y., Sun, Z., Zhang, Z., and Tong, H.: Effects of Agricultural
734 Large-And Medium-Sized Reservoirs on Hydrologic Processes in the Arid
735 Shiyang River Basin, Northwest China, *Water Resources Research*, 59,
736 e2022WR033519, <https://doi.org/10.1029/2022WR033519>, 2023.

737 Shastri, H., Paul, S., Ghosh, S., and Karmakar, S.: Impacts of urbanization on Indian
738 summer monsoon rainfall extremes, *J. Geophys. Res. Atmos.*, 120, 496–516,
739 <https://doi.org/10.1002/2014JD022061>, 2015.

740 Skrzypek, G., Mydłowski, A., Dogramaci, S., Hedley, P., Gibson, J. J., and Grierson,
741 P. F.: Estimation of evaporative loss based on the stable isotope composition of
742 water using Hydrocalculator, *Journal of Hydrology*, 523, 781–789,
743 <https://doi.org/10.1016/j.jhydrol.2015.02.010>, 2015.

744 Sun, G., Caldwell, P. V., and McNulty, S. G.: Modelling the potential role of forest
745 thinning in maintaining water supplies under a changing climate across the
746 conterminous United States: Response of Water Yield to Forest Thinning and
747 Climate Change, *Hydrol. Process.*, 29, 5016–5030,
748 <https://doi.org/10.1002/hyp.10469>, 2015.

749 Sun, G. and Lockaby, B. G.: Water Quantity and Quality at the Urban-Rural Interface,
750 in: *Urban-Rural Interfaces*, edited by: Laband, D. N., Lockaby, B. G., and
751 Zipperer, W. C., American Society of Agronomy, Soil Science Society of
752 America, Crop Science Society of America, Inc., Madison, WI, USA, 29–48,
753 <https://doi.org/10.2136/2012.urban-rural.c3>, 2012.

754 Sun, Z., Zhu, G., Zhang, Z., Xu, Y., Yong, L., Wan, Q., Ma, H., Sang, L., and Liu, Y.:
755 Identifying surface water evaporation loss of inland river basin based on
756 evaporation enrichment model, *Hydrological Processes*, 35, e14093,
757 <https://doi.org/10.1002/hyp.14093>, 2021.

758 Talma, S, Woodborne, S. and Lorentz, S.: South African Contribution to the Rivers
759 CRP, 2012.

760 UN-Habitat: World cities report 2020: the value of sustainable urbanization,
761 UN-Habitat, Nairobi, Kenya, 377 pp., 2020.

762 United Nations Department of Economic and Social Affairs: World Urbanization
763 Prospects 2018: Highlights, United Nations,
764 <https://doi.org/10.18356/6255ead2-en>, 2019.

765 Vitvar, T., Aggarwal, P. K., and Herczeg, A. L.: Global network is launched to

766 monitor isotopes in rivers, *Eos Trans. AGU*, 88, 325–326,
767 <https://doi.org/10.1029/2007EO330001>, 2007.

768 Vystavna, Y., Harjung, A., Monteiro, L. R., Matiatos, I., and Wassenaar, L. I.: Stable
769 isotopes in global lakes integrate catchment and climatic controls on evaporation,
770 *Nat Commun*, 12, 7224, <https://doi.org/10.1038/s41467-021-27569-x>, 2021.

771 Wang, B., Zhang, H., Liang, X., Li, X., and Wang, F.: Cumulative effects of cascade
772 dams on river water cycle: Evidence from hydrogen and oxygen isotopes,
773 *Journal of Hydrology*, 568, 604–610,
774 <https://doi.org/10.1016/j.jhydrol.2018.11.016>, 2019.

775 Wei, W., Shi, P., Zhou, J., Feng, H., Wang, X., and Wang, X.: Environmental
776 suitability evaluation for human settlements in an arid inland river basin: A case
777 study of the Shiyang River Basin, *J. Geogr. Sci.*, 23, 331–343,
778 <https://doi.org/10.1007/s11442-013-1013-y>, 2013.

779 Westra, S., Fowler, H. J., Evans, J. P., Alexander, L. V., Berg, P., Johnson, F.,
780 Kendon, E. J., Lenderink, G., and Roberts, N. M.: Future changes to the intensity
781 and frequency of short-duration extreme rainfall, *Rev. Geophys.*, 52, 522–555,
782 <https://doi.org/10.1002/2014RG000464>, 2014.

783 Wilson, C. and Weng, Q.: Assessing Surface Water Quality and Its Relation with
784 Urban Land Cover Changes in the Lake Calumet Area, Greater Chicago,
785 *Environmental Management*, 45, 1096–1111,
786 <https://doi.org/10.1007/s00267-010-9482-6>, 2010.

787 Wing, O. E. J., Bates, P. D., Smith, A. M., Sampson, C. C., Johnson, K. A., Fargione,
788 J., and Morefield, P.: Estimates of present and future flood risk in the
789 conterminous United States, *Environ. Res. Lett.*, 13, 034023,
790 <https://doi.org/10.1088/1748-9326/aaac65>, 2018.

791 Yang, L., Ni, G., Tian, F., and Niyogi, D.: Urbanization Exacerbated Rainfall Over
792 European Suburbs Under a Warming Climate, *Geophysical Research Letters*, 48,
793 e2021GL095987, <https://doi.org/10.1029/2021GL095987>, 2021.

794 Yang, S. L., Zhang, J., and Xu, X. J.: Influence of the Three Gorges Dam on
795 downstream delivery of sediment and its environmental implications, Yangtze
796 River, *Geophys. Res. Lett.*, 34, L10401, <https://doi.org/10.1029/2007GL029472>,
797 2007.

798 Yu, D., Shi, P., Liu, Y., and Xun, B.: Detecting land use-water quality relationships
799 from the viewpoint of ecological restoration in an urban area, *Ecological*
800 *Engineering*, 53, 205–216, <https://doi.org/10.1016/j.ecoleng.2012.12.045>, 2013.

801 Zhang, W., Wan, Q., Zhu, G., and Xu, Y.: Distribution of soil organic carbon and
802 carbon sequestration potential of different geomorphic units in Shiyang river
803 basin, China, *Environ Geochem Health*, 45, 4071–4086,
804 <https://doi.org/10.1007/s10653-022-01472-w>, 2023.

805 Zhu, G., Guo, H., Qin, D., Pan, H., Zhang, Y., Jia, W., and Ma, X.: Contribution of
806 recycled moisture to precipitation in the monsoon marginal zone: Estimate based
807 on stable isotope data, *Journal of Hydrology*, 569, 423–435,
808 <https://doi.org/10.1016/j.jhydrol.2018.12.014>, 2019.

809 Zhu, G., Sang, L., Zhang, Z., Sun, Z., Ma, H., Liu, Y., Zhao, K., Wang, L., and Guo,
810 H.: Impact of landscape dams on river water cycle in urban and peri-urban areas
811 in the Shiyang River Basin: Evidence obtained from hydrogen and oxygen
812 isotopes, Journal of Hydrology, 602, 126779,
813 <https://doi.org/10.1016/j.jhydrol.2021.126779>, 2021.